Ultraviolet Photodissociation Dynamics of 2-Methyl, 3-Furanthiol: Tuning π-Conjugation in Sulfur Substituted Heterocycles †

ARTICLE *in* THE JOURNAL OF PHYSICAL CHEMISTRY A · SEPTEMBER 2009

Impact Factor: 2.69 · DOI: 10.1021/jp905784f · Source: PubMed

4 AUTHORS, INCLUDING:

Tom Oliver
University of Bristol
39 PUBLICATIONS **636** CITATIONS
SEE PROFILE

Graeme King
VU University Amsterdam
22 PUBLICATIONS **450** CITATIONS
SEE PROFILE

Ultraviolet Photodissociation Dynamics of 2-Methyl, 3-Furanthiol: Tuning π-Conjugation in Sulfur Substituted Heterocycles†

Thomas A. A. Oliver, Graeme A. King, Michael G. D. Nix,‡ and Michael N. R. Ashfold*

School of Chemistry, University of Bristol, Bristol, BS8 1TS, U.K.

Received: June 19, 2009; Revised Manuscript Received: August 3, 2009

H atom loss following ultraviolet photoexcitation of 2-methyl, 3-furanthiol (2M,3FT) at many wavelengths in the range 269 nm $\geq \lambda_{phot} \geq$ 210 nm and at 193 nm has been investigated by H (Rydberg) atom photofragment translational spectroscopy. The photodissociation dynamics of this SH decorated aromatic ring system are contrasted with that of thiophenol (Devine et al. *J. Phys. Chem. A* **2008**, *112*, 9563), the excited electronic states of which show a different energetic ordering. *Ab initio* theory and experiment find that the first excited state of 2M,3FT is formed by electron promotion from an orbital comprised of an admixture of the S lone pair and the furan π system (n/π) to a σ^* orbital centered on the S−H bond. Photoexcitation at long wavelengths results in population of the $^1(n/\pi)\sigma^*$ excited state, prompt S−H bond fission, H atoms displaying a (nonlimiting) perpendicular recoil velocity distribution, and partner radicals formed in selected low vibrational levels of the ground state. This energy disposal can be rationalized by considering the forces acting as the excited molecules evolve on the $^1(n/\pi)\sigma^*$ potential energy surface (PES). Energy conservation arguments, together with the product vibrational state analysis, yield a value of 31320 ± 100 cm^{-1} for the S−H bond strength in 2M,3FT. Excitation at shorter wavelengths ($\lambda_{phot} \leq$ 230 nm) is deduced to populate one or more (diabatically bound) $^1(n/\pi)\pi^*$ excited states which decay by coupling to the $^1(n/\pi)\sigma^*$ PES and/or to high vibrational levels of the electronic ground state.

1. Introduction

Fast, dynamic, and direct X−H bond fission (where X is a heteroatom: N, O, or S) has been observed following ultraviolet (UV) photoexcitation of a wide range of heteroaromatic molecules, by detection of translationally excited H atom products. Illustrative examples include phenol[1−4] and substituted phenols,[1] thiophenol,[5−7] pyrrole,[8−10] imidazole,[11] indole,[12] and adenine.[13] The eventual dissociation in each case occurs on an excited $^1\pi\sigma^*$ state potential energy surface (PES). $\sigma^* \leftarrow \pi$ excitations typically have small oscillator strengths and the resulting $^1\pi\sigma^*$ excited states are thus often described as being "optically dark". In the cases of imidazole and pyrrole, the $^1\pi\sigma^*$ state is the first excited singlet state, which can be accessed directly by photon absorption, resulting in direct N−H bond fission. The $\sigma^* \leftarrow \pi$ excitation in the former molecule is electronically allowed, but the $^1A'' \leftarrow \tilde{X}^1A'$ transition has a small absorption cross section. Pyrrole has higher symmetry (C_{2v}) and $\sigma^* \leftarrow \pi$ excitation is electric dipole forbidden, but the $^1A_2 \leftarrow \tilde{X}^1A_1$ transition gains some absorption strength by vibronic induction. Multireference *ab initio* calculations[14] for these first-row heteroaromatic molecules show that, in each case, the $^1\pi\sigma^*$ states have some 3*s* Rydberg character in the vertical Franck−Condon region, that acquire progressively greater σ^*_{X-H} antibonding character upon extending R_{X-H} and correlate asymptotically to ground state radical products (plus an H atom). The ground state parent molecules, in contrast, correlate diabatically with an excited state of the radical product, thereby yielding a conical intersection (CI) between the ground and excited ($^1\pi\sigma^*$) PESs in the X−H bond dissociation coordinate. Phenols, indole, and adenine each have C_s (or quasi-C_s) symmetry, and their first excited $^1\pi\pi^*$ state(s) lie at energies below the $^1\pi\sigma^*$ state. UV photoexcitation of these molecules populates mainly (if not exclusively) the optically bright $^1\pi\pi^*$ state(s), which can decay via nonadiabatic coupling to the $^1\pi\sigma^*$ PES (at another, higher energy, CI) and subsequent X−H bond fission.

The present study focuses on a thiofuran, which contains another class of heteroaromatic chromophore. Given that this molecule involves an SH group attached to a planar aromatic ring, we might anticipate photochemical similarities with that of thiophenol.[5−7] Furan is less aromatic than benzene, and its π electron density is distributed unevenly around the ring; both factors influence the extent to which this π density mixes with the lone pair (n) on the pendant S atom.

The electronic structure and the excited states of bare furan have been studied extensively, both experimentally[15−21] and theoretically.[22−27] *Ab initio* calculations identify the highest occupied molecular orbitals (HOMOs) of furan as two π orbitals, of b_1 and a_2 symmetry, and the lowest unoccupied molecular orbitals (LUMOs) as two π^* orbitals, again with b_1 and a_2 symmetry. Resonance enhanced multiphoton ionization (REMPI)[15,17] studies revealed the one photon forbidden, two photon allowed $^1A_2(3s) \leftarrow \pi(a_2)$ Rydberg state of furan at an energy of $E \sim$5.91 eV. Electron energy loss[15] and vacuum UV (VUV) absorption[18] spectroscopy studies support the earlier REMPI studies in locating the first $^1\pi\pi^*$ valence state, the $^1B_2(b_1 \leftarrow a_2)$ state, at $E \sim$6.06 eV. The assignment of vibronic structure observed in these spectra at higher energies (6.47 eV $< E <$ 6.76 eV) had been a source of some controversy,[17] but subsequent *ab initio* calculations[25,27] identify three electronic origins in this region in order of increasing energy; the

† Part of the "W. Carl Lineberger Festschrift".

* To whom correspondence should be addressed. E-mail: mike.ashfold@bristol.ac.uk. Phone: +44 (117) 928 8312. Fax: +44 (117) 925 0612.

‡ Current address: Department of Chemistry, University of York, York, YO10 5DD.

10.1021/jp905784f
Published on Web 08/25/2009

$^1B_1(3p_y \leftarrow a_2)$, $^1A_2(3p_z \leftarrow a_2)$, and $^1B_2(3p_x \leftarrow a_2)$ Rydberg transitions. Two states of $^1A_1$ symmetry, arising from the $a_2 \leftarrow a_2$ and $b_1 \leftarrow b_1$ valence excitations and labeled $^1A_1^+$ and $^1A_1^-$, are identified at $E \sim 7.8$ eV. Calculations associate most of the observed oscillator strength at this energy with transition to the higher energy $^1A_1^+$ state.[22,25]

The photodissociation of furan at $\lambda_{phot} = 193$ nm has been investigated by photofragment translational spectroscopy (PTS) methods, using tunable VUV radiation to ionize the resulting fragments.[21] Three fragmentation pathways were identified. Two, yielding $C_2H_2O + C_2H_2$ and $CO + C_3H_4$ products with low kinetic energies and isotropic recoil velocity distributions, were attributed to the unimolecular decay of highly vibrationally excited ground state molecules, formed following internal conversion from the excited state populated by photon absorption. The third pathway yielded the radical products $HCO + C_3H_3$ (propargyl), with substantial kinetic energy (~25% of the available energy) and an anisotropic distribution of recoil velocities. Such dynamic (nonstatistical) energy disposal implies that this dissociation occurs on an excited state PES. Sorkabi et al.[21] suggested initial excitation to a $^1B_2(^1\pi\pi^*)$ state, radiationless transfer to a ring-opening excited state formed by cleaving one C−O bond, and subsequent H-atom transfer, all on a time scale faster than molecular rotation. Optimized time dependent density functional theory (TD-DFT) calculations[26] lend support to aspects of this mechanism, predicting that ring opening by C−O bond cleavage becomes a competitive channel once $E \sim 6.1$ eV. The calculations suggest that the initial excitation is to the $^1B_2(^1\pi\pi^*)$ state, which couples to the ring-opening $^1B_1(^1\pi\sigma^*)$ state (promoted by appropriate out-of-plane bending motions) via a CI linking these two PESs. Importantly for the present studies, none of the available data suggests any significant production of H atom fragments following UV photoexcitation of furan.

Substituting an SH group at the 3-position (defined relative to the O atom in furan) gives 3-furanthiol (3FT). 3FT is unstable, however, preferring to exist as the thioketo tautomer (which we calculate to be ~135 cm^{-1} lower in energy than the thiol). Such tautomerism can be prevented by substituting a methyl group in the 2-position, giving 2-methyl, 3-furanthiol (2M,3FT, alternatively named 2-methyl-3-mercaptofuran). This molecule involves a planar ring, but as shown later, the minimum energy structure has the S−H bond directed near perpendicular to the ring plane. 2M,3FT is formed by the reaction of ribose and cysteine, is often detected in cooked meats, and thus finds use as a flavoring in the food industry.[28]

The closest analogue of 2M,3FT that has been subject to any detailed spectroscopic study is 2-methylfuran (2MF), for which both UV absorption[29] and REMPI[30] spectra have been reported. The π system appears to be only slightly perturbed by addition of the methyl group, but the associated inductive effect lowers the ionization potential, and the energies of the Rydberg states and series that converge to this limit, by ~0.5 eV relative to bare furan. The energies of the valence excited states, in contrast, are little affected by methyl substitution at the 2-position, showing red-shifts of only ~0.1 eV relative to the corresponding excitations in furan.

Here we report time-of-flight (TOF) spectra of the H atoms released upon photolysis of jet-cooled 2M,3FT molecules at many different wavelengths in the range 210 nm $\leq \lambda_{phot} \leq$ 269 nm and at 193 nm, by use of the H (Rydberg) atom (HRA)-PTS technique.[10,31] The structure observed in these TOF spectra is attributed to S−H bond fission, with formation of the partner 2-methyl, 3-furanthiyl (2M,3FTyl) radical in a very limited subset of its available vibrational states. The derived S−H bond strength and product energy disposals are compared with those measured following UV photolysis of thiophenol. Evident similarities and differences are discussed in terms of the relative energetics of the $^1(n/\pi)\sigma^*$ and $^1(n/\pi)\pi^*$ PESs in these two molecules, and the extents of mixing between the ring π electrons and the S lone pair.

2. Experimental Section

2M,3FT was purchased from Sigma Aldrich (85% purity) and used without further purification. As we show later (Figures 4 and 5), the main impurity is deduced to be the thioketo tautomer of 3FT. The HRA-PTS experimental apparatus has been detailed previously.[10] Briefly, a sample of 2M,3FT (room temperature vapor pressure, seeded in ~700 Torr of argon) was expanded into a vacuum through a pulsed valve (General Valve Series 9) and skimmed to form a cold molecular beam. This molecular beam was intersected by a photolysis pulse generated by frequency doubling the output of a Nd:YAG pumped dye laser (Spectra Physics GCR-270 plus PDL-2, 269 nm $\geq \lambda_{phot} \geq$ 210 nm, ~0.5−2 mJ $pulse^{-1}$) or with an ArF laser (Lambda-Physik OpteX, 193 nm, ~1−2 mJ $pulse^{-1}$). The precise wavelength of the former radiation was measured by directing a portion of the fundamental dye laser output into a wavemeter (Coherent Wavemaster). The UV radiation was focused into the interaction region using an $f = 75$ cm lens. After a time delay of $\delta t = 10$ ns, H atom photoproducts in the interaction region were tagged using a doubly resonant two photon excitation scheme involving, first, Lyman-α (121.6 nm) excitation to the $2p$ state, followed by excitation at ~366 nm to a high n Rydberg state ($n \sim 80$). The requisite tagging photons were created using two separate dye lasers pumped by the second harmonic of a single Nd:YAG laser (Continuum Powerlite 9010). The Lyman-α radiation was produced by mixing the 554.782 nm output of one dye laser with residual 1064 nm radiation to produce light of wavelength 364.7 nm, which was then focused in a cell containing a phase matched Kr/Ar gas mixture. The resulting 121.6 nm radiation is then refocused into the interaction region (MgF_2 lens). Any prompt ions formed from unintentional VUV or multiphoton induced ionization processes were removed by biasing (20 V cm^{-1}) an extractor plate assembly that straddled the interaction region. Tagged H (Rydberg) atoms with recoil velocities along the TOF axis travel to a Johnston multiplier detector (held at −4.2 kV) where they are field ionised and their arrival time recorded.

The length of the TOF axis used in these experiments, d (~37.1 cm), was frequently recalibrated by recording TOF spectra of H atoms resulting from H_2S photodissociation at $\lambda_{phot} <$ 240 nm, and least-squares fitting to well-characterized spin−orbit resolved peaks associated with the H + SH (X, v, N) product channels, using the literature value for $D_0(H-SH)$[31,32] and the relevant diatomic term values.[33] The electric polarization vector, $\boldsymbol{\varepsilon}_{phot}$, of the photolysis laser radiation was ordinarily aligned at an angle of $\theta = 90°$ to the TOF axis. When necessary, $\boldsymbol{\varepsilon}_{phot}$ could be rotated by inserting a double Fresnel rhomb (Optics for Research). As before,[32] TOF (and thus kinetic energy) dependent recoil anisotropy parameters, β, were determined by recording spectra with $\boldsymbol{\varepsilon}_{phot}$ aligned at $\theta = 0$, 54.7, and 90°.

REMPI of the 2M,3FT sample (and its principal impurities) was investigated by substituting a (removable) Wiley-McClaren TOF-mass spectrometer (MS) in place of the extractor plate. Ion TOF spectra recorded at a fixed λ_{phot} revealed the dominant m/z peaks. Monitoring a particular m/z signal while scanning

λ_{phot} yielded REMPI excitation spectra of the target species. Photofragment excitation (PHOFEX) spectra for forming H^+ ions were sought also, by introducing the Lyman-α laser pulse (along with the 364.7 nm fundamental from which it is derived, at $\delta t \sim 10$ ns) and scanning λ_{phot}.

3. Computational Methods

Ground state geometry optimizations and vibrational frequencies (with anharmonic corrections) for 2M,3FT and the 2M,3FTyl radical were calculated using DFT and the hybrid functional B3LYP with a Pople basis set, of triple-ζ quality: 6-311+G** in the Gaussian 03 suite.[34] Natural bonding orbital (NBO) analyses were also performed in Gaussian 03, to aid understanding of the nonplanarity of 2M,3FT.

Complete active space self consistent field (CASSCF) calculations were performed in Molpro, version 2006.1,[35] using a 10/9 active space consisting of two π orbitals, the S lone pair, C−S σ and ring σ orbitals, and virtual orbitals comprising two π^* furan orbitals, and S−H and C−S σ^* orbitals. Dunning's augmented correlation consistent basis set of triple-ζ quality: aug-cc-pVTZ, was used. The ground and first three excited states of 2M,3FT were optimized at the ground state equilibrium value of R_{S-H} (1.395 Å), and at many other R_{S-H} distances. CASPT2 single point energies were then taken at these optimized geometries (freezing the carbon and oxygen 1*s* electrons and the sulfur 1*s* and 2*s* electrons). Intruder state problems were encountered in the CASPT2 calculations, preventing convergence. Such problems are typically due to low lying, diffuse (Rydberg) virtual orbitals omitted from the active space interacting with the near degenerate reference excited state. A small imaginary level shift, as described by Roos and Andersson,[36] was required to circumvent this problem, enabling convergence.

TD-DFT methods are finding increasing use as a means of characterizing excited states of molecules like imidazole,[37] furan,[26] and pyrrole[38] and were also used here as an alternative to the CASSCF//CASPT2 approach. All TD-DFT calculations were performed in Turbomole;[39] ground and excited states were optimized using the B3LYP functional with the def2-TZVP and TZVP basis sets.

4. Results

4.1. Computational Results. Optimization of the ground state geometry of 2M,3FT with both DFT/B3LYP/6-311+G** and CASSCF(10/9)/aug-cc-pVTZ reveals that the furan ring remains planar but the S−H bond lies out of the ring plane, with a C−C−S−H dihedral angle of $\phi = 72.8°$, as shown in Figure 1a. This configuration, in which the S lone pair is aligned nearly perpendicular to the π system of the furan ring, is calculated (at the B3LYP/6-311+G** level) to be ~690 cm^{-1} lower in energy than the planar ($\phi = 0°$) geometry. The methyl rotational barrier (31 cm^{-1}, again calculated at the B3LYP/6-311+G** level) is sufficiently small for the pendant CH_3 group to be treated as a free rotor.

The nonplanarity of 2M,3FT cannot be wholly explained on steric grounds. Equivalent calculations on 3FT show that it, too, favors a nonplanar equilibrium geometry, with a barrier to S−H torsional motion of ~440 cm^{-1} (cf. ~810 cm^{-1} in 2M,3FT). It is well established that the aromaticity of the five-membered heteroycles decreases along the series: thiophene > pyrrole > furan,[40] a finding that is generally explained in terms of reduced electron delocalization (i.e., reduced donation of the lone pair density associated with the heteroatom to the rest of the ring). Thus, the π system in furan is often alternatively pictured in terms of a lone pair (on O) and two localized double bonds.

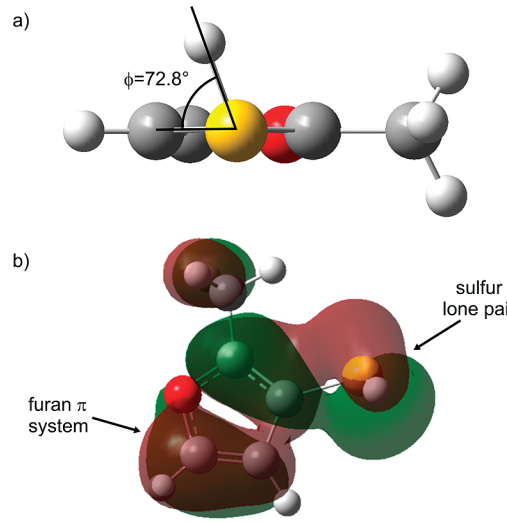

Figure 1. (a) View down the C−S bond illustrating the C−C−S−H dihedral angle, ϕ, for 2M,3FT at the ground state equilibrium geometry. (b) HOMO of 2M,3FT: an admixture of the S lone pair orbital, *n*, and the ring π system.

NBO analyses, whereby delocalized MOs are transformed into Lewis-acid-like localized orbitals, can offer some insight into conjugative effects, as demonstrated in a recent study of hyperconjugation in ethanol conformers.[41] Application of NBO analysis to 2M,3FT shows the S lone pair orbital conjugating into the ring structure when $\phi = 0°$, thereby lowering the energy of the lone pair orbital. This energetic benefit is outweighed by the simultaneous increase in the energies of the C=C π orbitals and of the O atom lone pair, however, which manifests itself via a lengthening of the C(2)—C(3) and C(4)—C(5) double bonds and some reduction of the C(3)—C(4) bond length. Conjugating the S lone pair thus causes a net destabilization of the furan ring system and the 2M,3FT molecule. Some conjugation is clearly beneficial, however, given that the minimum energy configuration involves $\phi = 72.8°$ (rather than $\phi = 90°$ which would align the S lone pair completely orthogonal to the ring π system). Such behavior is not unique to 2M,3FT and 3FT. Similar calculations (at the B3LYP/6-311+G** level) predict 3-thiopyrrole to have a similarly nonplanar ground state equilibrium geometry but that 3-hydroxyfuran and 3-hydroxypyrrole are planar, reflecting the reduced tendency for electron donation from the more electronegative O (in OH) to the five-membered ring.

CASSCF/CASPT2 (and TD-DFT) calculations predict that the lowest energy (singlet) transition connects the HOMO, which, as Figure 1b shows, is a complicated admixture of the S lone pair orbital, *n*, and the ring π system (henceforth labeled n/π), to a LUMO that (after relaxing the excited state geometry) is well-described as a σ^* orbital localized on the S−H bond. The calculated (TD-DFT) transition moment lies roughly in the plane defined by the C−S−H group, such that it intersects the S−H bond at an angle of ~50°. The second and third excited singlet states are both calculated to be bound $^1(n/\pi)\pi^*$ states. Both CASSCF and TD-DFT methods indicate that the $^1(n/\pi)\sigma^*$ and $^1(n/\pi)\pi^*$ excited states have planar geometries (i.e., $\phi = 0°$) at the ground state value of R_{S-H}. This can be rationalized by recognizing that the electronic excitations create a "hole" in the π ring system that will be stabilized by increased conjugation with the S lone pair (such as is achieved when $\phi = 0°$). The two sets of calculations give the same energetic ordering of these excited states, but as Table 1 shows, TD-DFT predicts significantly lower excitation energies in all cases.

TABLE 1: Calculated Zero-Point Energy Corrected Optimized Excitation Energies (at the Ground State Equilibrium R_{S-H} Value) Comparing CASSCF(10/9)// CASPT2(10/9)/aug-cc-pVTZ and TD-DFT with TZVP and def2-TZVP Basis Sets

	optimized excitation energy/eV		
state	CASSCF(10/9)// CASPT2(10/9)/ aug-cc-pVTZ	TD-DFT/ TZVP	TD-DFT/ def2-TZVP
$^1(n/\pi)\sigma^*$	4.66	4.20	4.09
$^1(n/\pi)\pi^*$	5.83	5.02	4.42
$^1(n/\pi)\pi^*$	6.14	5.52	4.95

Figure 2 displays cuts (along R_{S-H}) through potentials for the ground and first three excited singlet states of 2M,3FT calculated with CASSCF(10/9)//CASPT2(10/9)/aug-cc-pVTZ. The energetic benefit achieved by misaligning the S lone pair and the ring π system in the ground state declines with increasing R_{S-H}, and by $R_{S-H} \sim 2.5$ Å, the minimum energy configuration has the S−H bond lying in the plane of the furan ring, thus acquiring A' (C_s) symmetry. As Figure 2 shows, upon extension of R_{S-H}, the ground state correlates (diabatically) with 2M,3FTyl fragments in their first excited ($\tilde{A}^2A'$) state, while the $^1(n/\pi)\sigma^*$ potential dissociates to ground ($\tilde{X}^2A''$) state fragments, and the two PESs are linked by a CI at $R_{S-H} \sim 2.9$ Å. Both states of the 2M,3FTyl radical are calculated to have planar equilibrium geometries. Geometry differences between the heavy atom frames of ground state 2M,3FT and 2M,3FTyl are minor, though H atom loss is seen to be accompanied by some modest ring expansion, most notably an expansion of the C(2)−C(3) bond (~3%) and reduction of the C(4)−C(5) bond (~2%). CASSCF//CASPT2 calculations give a 2M,3FTyl($\tilde{A}^2A'-\tilde{X}^2A''$) separation of 5110 cm^{-1}, somewhat larger than the corresponding splitting for the thiophenoxyl radical (2800 ± 40 cm^{-1}).[7] This increased splitting can be traced to greater conjugation between the S $3p_x$ orbital and the π orbital associated with the C(2)−C(3) bond in the ground ($\tilde{X}^2A''$) state radical; as in thiophenoxyl, the singly occupied molecular orbital (SOMO) in the $\tilde{A}^2A'$ state radical is predominantly the S $3p_y$ orbital.

4.2. UV Absorption, Photoionisation Mass Spectrometry, and REMPI Spectroscopy of 2M,3FT. As Figure 3 shows, the room temperature UV absorption of 2M,3FT shows an onset

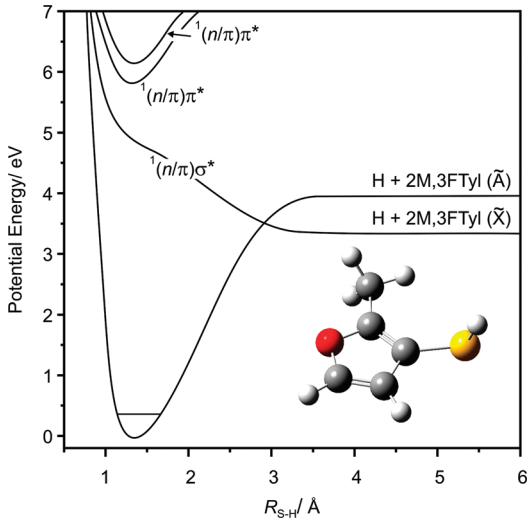

Figure 2. Sections, along R_{S-H}, through the calculated (CASPT2(10/9)/aug-cc-pVTZ) PESs for the ground and first three singlet excited states of 2M,3FT; see text for details.

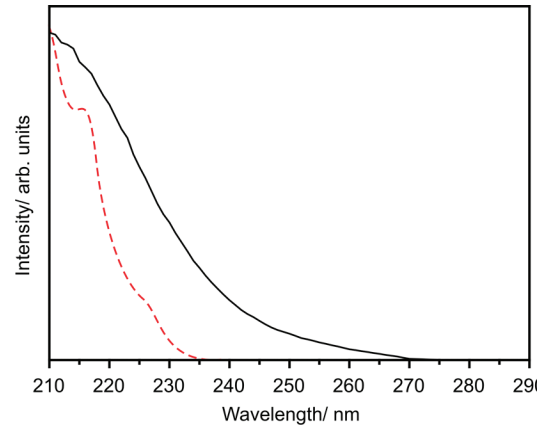

Figure 3. Room temperature UV absorption spectrum of 2M,3FT (black line) and 2MF (red line, adapted from ref 29) over the wavelength range 210 nm ≤ λ_{phot} ≤ 290 nm.

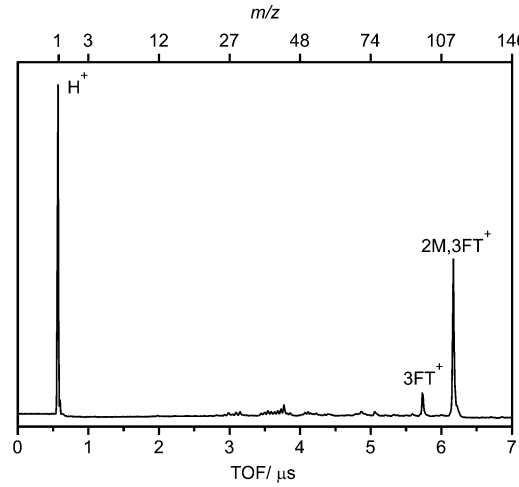

Figure 4. Ion TOF-mass spectrum obtained following excitation of the jet-cooled 2M,3FT sample at λ_{phot} = 265 nm, with the Lyman-α radiation (and the 364.7 nm radiation from which it derives) present after $\delta t \sim 10$ ns.

at ~270 nm and increases with decreasing λ_{phot}. The absorption limits for furan and 2MF occur at significantly shorter wavelengths, ~230[18] and ~240 nm,[29] respectively. For comparison purposes, the absorption spectrum of 2MF is included in Figure 3, with both spectra arbitrarily scaled to the same peak intensity at 210 nm. The strong absorptions in furan and 2MF are assigned to $\pi^* \leftarrow \pi$ transitions. Addition of an SH moiety in the 3-position reduces the energies of the $\pi^* \leftarrow \pi$ (or here $\pi^* \leftarrow n/\pi$) transitions further. Additionally, and more importantly in the present context, it introduces an extra shoulder at long wavelength, attributable to the $\sigma^* \leftarrow n/\pi$ excitation.

The REMPI TOF-mass spectrum recorded at λ_{phot} = 265 nm is dominated by the parent ion peak (m/z 114) with a much smaller feature at m/z 100. The latter is likely attributable to ionization of the (assumed) 3FT impurity in the as supplied 2M,3FT sample. Introducing the Lyman-α radiation (along with the 364.7 nm radiation from which it derives) after $\delta t \sim 10$ ns leads to an additional peak at m/z 1, attributable to two-color resonant ionization of neutral H atoms, as shown in Figure 4. Excitation spectra for forming ions with m/z 114, 100, and (after introducing Lyman-α radiation) 1 were recorded across the range 260 nm ≤ λ_{phot} ≤ 280 nm. Neither the parent ion signal nor the H atom PHOFEX spectrum displayed any wavelength dependence, but the m/z 100 signal exhibited a structured REMPI spectrum, as shown in Figure 5. The relative simplicity

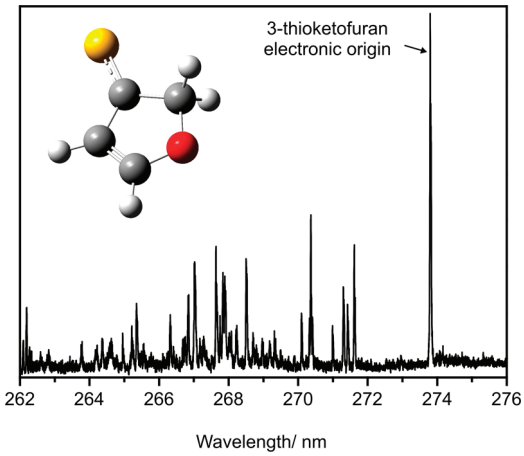

Figure 5. REMPI excitation spectrum for forming ions with m/z 100 recorded in the wavelength range 262 nm $\leq \lambda_{phot} \leq$ 276 nm, attributed to the thioketo tautomer of 3FT.

of this spectrum reinforces the view that the m/z 100 signal is from a jet-cooled impurity in the parent beam, and the absence of any comparable structure in the H atom PHOFEX spectrum supports the view that this impurity (with electronic origin at 273.799 nm) is the thioketo tautomer of 3FT, in which S−H fission is not possible.

Electronic structure calculations, the form of the UV absorption spectrum, and the lack of any structure in the REMPI excitation spectrum for forming ions with m/z 114 all point to the fact that the first excited state of 2M,3FT is the $^1(n/\pi)\sigma^*$ state and that it is dissociative with respect to R_{S-H}.

4.3. H (Rydberg) Atom Photofragment Translational Spectroscopy. H atom TOF spectra were recorded following excitation at many wavelengths in the range 269 nm $\geq \lambda_{phot} \geq$ 210 nm and at 193 nm. The H atom TOF spectra were converted into total kinetic energy released (TKER) spectra using eq 1:

$$\mathrm{TKER} = \frac{1}{2} m_H \left(1 + \frac{m_H}{m_R}\right)\left(\frac{d}{t}\right)^2 \quad (1)$$

where m_H is the mass of the hydrogen atom (1.00794 u) and m_R is the mass of the assumed cofragment, 2M,3FTyl (113.1576 u), d is the distance between the interaction region and the detector, and t the TOF for a given H atom to arrive at the detector. A t^{-3} Jacobian is used to rebin the intensities when converting measured TOF spectra into TKER spectra.

Figure 6 shows representative TKER spectra measured at four different excitation wavelengths within the range 269 nm $\geq \lambda_{phot} \geq$ 210 nm. The longest wavelength at which a TKER spectrum could be obtained was $\lambda_{phot} = 269.0$ nm. This spectrum (Figure 6a) is dominated by a structured feature at TKER ~4500 cm^{-1}, with some signal at lower TKER, consistent with formation of radical fragments with higher internal (vibrational) excitation. Photolysis at shorter wavelengths ($\lambda_{phot} = 255.0$ nm, Figure 6b) yields a similar spectrum, though the fast peak has shifted to higher TKER by an amount equal to the increase in the photon energy. The sharp onset at high TKER is still apparent in the spectrum obtained at $\lambda_{phot} = 230.0$ nm (at TKER ~12000 cm^{-1}, Figure 6c), but the proportion of "slow" signal (centered at ~2000 cm^{-1}) is now greater, and an additional maximum is evident at TKER ~7500 cm^{-1}. By $\lambda_{phot} = 210.0$ nm (Figure 6d) and at 193 nm (not shown), the peak at low TKER is dominant, but the fast onset is still apparent (at TKER ~16000 cm^{-1} in Figure 6d).

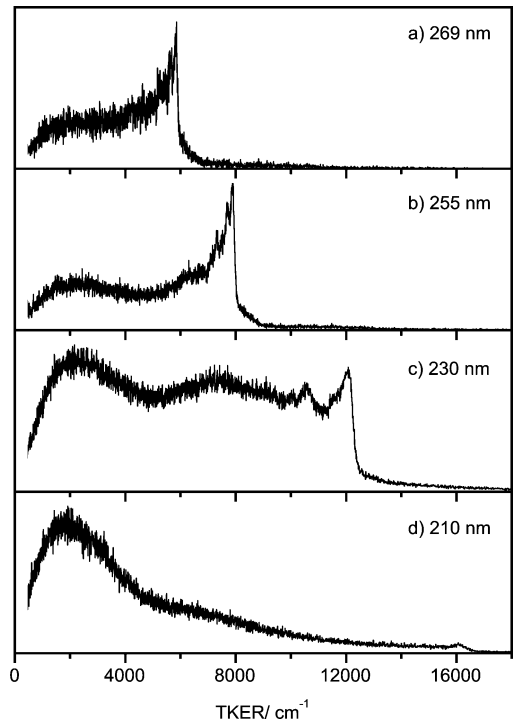

Figure 6. TKER spectra derived from H atom TOF spectra measured at λ_{phot} = (a) 269.0 nm, (b) 255.0 nm, (c) 230.0 nm, and (d) 210.0 nm measured with $\boldsymbol{\varepsilon}_{phot}$ aligned at $\theta = 90°$ to the TOF axis.

The structured features at high TKER appear most clearly when $\boldsymbol{\varepsilon}_{phot}$ is aligned perpendicular to the TOF axis. Careful measurements at $\lambda_{phot} = 253.0$ and 240.0 nm, whereby TOF spectra measured with $\boldsymbol{\varepsilon}_{phot}$ aligned at $\theta = 0$, 54.7, and 90° are subsequently normalized, summed, and appropriately ratioed,[32] reveal that the fast, structured features have an associated recoil anisotropy parameter, $\beta \sim -0.5$. The observations that β at these TKER values is nonzero, and negative, are consistent with the earlier conclusions: (i) that these fast H atoms arise as a result of direct photoexcitation to the $^1(n/\pi)\sigma^*$ state, which undergoes S−H bond fission directly, on a time scale that is faster than the parent rotational period, and (ii) that the $\sigma^* \leftarrow (n/\pi)$ transition moment is aligned at an angle to the breaking S−H bond.

Energy conservation requires that

$$E_{phot} + E_{int}(\mathrm{2M,3FT}) = \mathrm{TKER} + D_0(\mathrm{H–2M,3FTyl}) + E_{int}(\mathrm{2M,3FTyl}) \quad (2)$$

where E_{int}(2M,3FT) and E_{int}(2M,3FTyl) are, respectively, the internal energies of the parent (traditionally approximated as zero in a jet-cooled sample) and the radical product and D_0(H–2M,3FTyl) is the S−H bond strength. There is no *a priori* reason why dissociation from the $^1(n/\pi)\sigma^*$ state should favor formation of product states of any particular vibrational symmetry, so we associate the peak at highest TKER in each spectrum to formation of H + 2M,3FTyl($\tilde{X}^2A''$) products in their ground ($v = 0$) level, (i.e., with E_{int}(2M,3FTyl) = 0) and thereby derive D_0(H–2M,3FTyl) = 31320 ± 100 cm^{-1} from analysis of spectra measured at 13 different photolysis wavelengths. The larger uncertainty (±100 cm^{-1}) associated with the recommended value for D_0(H–2M,3FTyl) recognizes two factors: (i) the uncertainty in estimating the TKER value associated with $v = 0$ products (given the possible population of the low frequency CH_3 torsional levels in the product) and (ii) by

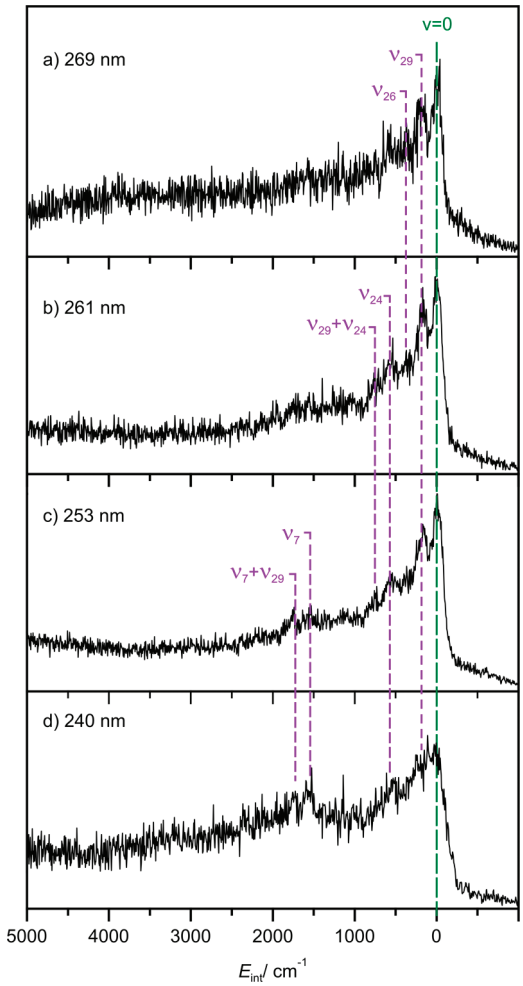

Figure 7. Internal energy spectra of 2M,3FTyl radicals formed by photolysis at λ_{phot} = (a) 269.0 nm, (b) 261.0 nm, (c) 253.0 nm, and (d) 240.0 nm. Individual peaks have been assigned by reference to the calculated anharmonic wavenumbers listed in Table 2.

analogy with thiophenol,[7] the possibility that the SH (and/or CH_3) torsional modes in the jet-cooled parent molecule may not have cooled completely (i.e., that the E_{int}(2M,3FT) ~0 approximation may not be wholly valid).

Given D_0(H–2M,3FTyl), eq 2 can be rearranged so that TKER spectra can be recast in terms of the radical internal energy, thereby allowing determination and analysis of the product vibrational energy disposal and its variation with λ_{phot}. Illustrative E_{int}(2M,3FTyl) spectra are shown in Figure 7. Note that the above energetic uncertainties mostly compromise the determination of absolute TKER values, and thus D_0(H–2M,3FTyl). The energy differences *between* peaks in a TKER spectrum are determined to much greater precision. Assignment of the partially resolved structure evident in these spectra is guided by reference to the calculated (anharmonic corrected) wavenumbers of the normal modes of vibration of the ground state 2M,3FTyl radical listed in Table 2.

The structure observed at long λ_{phot} is most simply assigned to the formation of 2M,3FTyl products in their $v = 0$ level, and in levels carrying one quantum of ν_{29} (an out-of-plane wag), ν_{26} (a combined C−S wag and ring-twist motion), ν_{24} (an out-of-plane ring twist), and combinations thereof (see Figure 7a and b). The normal mode displacements associated with these low frequency modes are shown in Figure 8. Activity in each of these modes can be rationalized, qualitatively, by considering the effect of the impulse imparted to the S end of the C−S

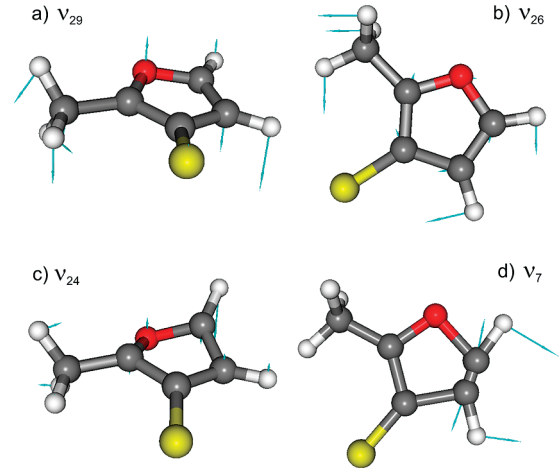

Figure 8. Nuclear motions associated with 2M,3FTyl radical modes populated in the long wavelength photolysis of 2M,3FT: (a) ν_{29}, out-of-plane flapping motion of the ring; (b) ν_{26}, combined C−S wag and in-plane ring twist; (c) ν_{24}, out-of-plane ring twist; (d) ν_7, in-plane stretch centered on the C(4) and C(5) atoms.

bond by the H atom departing at an angle that is far from collinear and, initially at least, far from coplanar. Population of one additional, higher frequency product mode (ν_7) is identified in spectra recorded at λ_{phot} = 253.0 nm (Figure 7c) and, particularly, 240.0 nm (Figure 7d). As Figure 8 shows, product mode ν_7 is a localized stretching motion centered on the C(4)−C(5) bond. Activity in this mode can be understood by recalling the changes in equilibrium geometry of the heavy atom frame as a result of photoexcitation and the subsequent evolution to the eventual radical product, as discussed in section 4.1. A similar C−C ring stretching motion was identified in the imidazolyl products resulting from $\sigma^* \leftarrow \pi$ excitation in imidazole, and rationalized by analogous Franck−Condon considerations.[11]

The fraction of the available energy (i.e., $E_{phot} - D_0$(H–2M,3FTyl)) appearing as product translation falls with decreasing λ_{phot} (increasing E_{phot}). TKER spectra obtained at λ_{phot} = 230.0 nm (Figure 6c), and at neighboring wavelengths, show a secondary maximum with TKER ~7500 cm^{-1}. Given the predicted energy separation of the $\tilde{A}^2A'$ and $\tilde{X}^2A''$ states of the 2M,3FTyl radical (~5110 cm^{-1} from the CASPT2 calculations), it is tempting to associate this maximum with formation of 2M,3FTyl($\tilde{A}^2A'$) products.

Prior UV photoexcitation studies of methanethiol[42] have demonstrated the operation of a competing C−S bond fission pathway, both by direct observation of the SH fragments[43] and by observing H atoms resulting from secondary photolysis of these SH(X) products.[42] C−S bond fission has also been reported in the 193 nm photolysis of thiophenol.[44] Clearly, such bond fission could be a primary photofragmentation pathway in 2M,3FT also, and the present *ab initio* calculations confirm that the process is energetically feasible. H atom TOF spectra measured at $\lambda_{phot} \leq$ 220 nm were examined particularly carefully for features that might be attributable to secondary photolysis of primary SH(X) products from a rival C−S bond fission, but no clear evidence for any such H atoms was discerned.

5. Discussion

Attachment of an SH group to furan, rather than to a benzene ring as in thiophenol, alters the relative disposition of the $^1(n/\pi)\sigma^*$ and $^1(n/\pi)\pi^*$ states such that it becomes possible to populate the $^1(n/\pi)\sigma^*$ state directly, and to monitor the

TABLE 2: Calculated Harmonic and Anharmonic Corrected Vibrational Wavenumbers (cm^{-1}) for 2M,3FT and the 2M,3FTyl Radical[a]

2M,3FT ($\tilde{X}^1A$)				2M,3FTyl($\tilde{X}^2A''$)			
mode	symmetry	harmonic	anharmonic	mode	symmetry	harmonic	anharmonic
ν_1	a	3280	3145	ν_1	a'	3283	3150
ν_2	a	3251	3128	ν_2	a'	3257	3122
ν_3	a	3129	2982	ν_3	a'	3136	2993
ν_4	a	3075	2927	ν_4	a''	3074	2921
ν_5	a	3028	2917	ν_5	a'	3026	2904
ν_6	a	2630	2512			Disappearing Mode	
ν_7	a	1619	1589	ν_6	a'	1510	1469
ν_8	a	1544	1510	ν_7	a'	1575	1542
ν_9	a	1483	1442	ν_8	a'	1453	1415
ν_{10}	a	1479	1441	ν_9	a''	1474	1434
ν_{11}	a	1419	1388	ν_{10}	a'	1403	1373
ν_{12}	a	1392	1362	ν_{11}	a'	1384	1351
ν_{13}	a	1235	1199	ν_{12}	a'	1251	1218
ν_{14}	a	1210	1188	ν_{13}	a'	1210	1188
ν_{15}	a	1149	1127	ν_{14}	a'	1120	1094
ν_{16}	a	1115	1057	ν_{15}	a'	1100	1078
ν_{17}	a	1064	1045	ν_{16}	a''	1043	1015
ν_{18}	a	1033	1016	ν_{17}	a'	1020	993
ν_{19}	a	955	936	ν_{18}	a'	957	941
ν_{20}	a	944	936			Disappearing Mode	
ν_{21}	a	908	897	ν_{19}	a'	886	872
ν_{22}	a	864	849	ν_{20}	a''	886	866
ν_{23}	a	741	720	ν_{21}	a''	766	749
ν_{24}	a	678	669	ν_{22}	a'	679	666
ν_{25}	a	641	638	ν_{23}	a''	656	649
ν_{26}	a	616	607	ν_{24}	a''	582	573
ν_{27}	a	477	472	ν_{25}	a'	511	506
ν_{28}	a	380	377	ν_{26}	a'	391	390
ν_{29}	a	251	253	ν_{27}	a''	261	261
ν_{30}	a	214	210	ν_{28}	a'	225	223
ν_{31}	a	198	170	ν_{29}	a''	185	184
ν_{32}	a	190	140			Disappearing Mode	
ν_{33}	a	107	78	ν_{30}	a''	100	122

[a] The parent modes are labeled following the Herzberg notation,[45] whereas the numbering of the 2M,3FTyl($\tilde{X}^2A''$) radical modes maps through from the corresponding normal modes of the parent molecule.

subsequent S−H bond fission. This process occurs on a time scale that is short compared to the parent rotational period, and proceeds through the CI with the ground state PES at large R_{S-H}, yielding 2M,3FTyl($\tilde{X}^2A''$) products in a very limited subset of the available vibrational states, the identities of which can be rationalized by considering the forces acting on the molecule during the photoexcitation and subsequent bond fission.

Electronic branching in the 2M,3FTyl radical products is determined by the extent of nonadiabatic coupling at the CI connecting the $^1(n/\pi)\sigma^*$ and ground state PESs at extended R_{S-H} (see Figure 2). Electronically excited molecules that approach this CI with planar configurations can be expected to follow the diabatic path, leading to ground $\tilde{X}^2A''$ state radical products, as observed at the longest λ_{phot}. Once $\lambda_{phot} \leq 230$ nm, the initial absorption increasingly populates the lowest $^1(n/\pi)\pi^*$ state, the subsequent dissociation of which requires initial radiationless transfer to the $^1(n/\pi)\sigma^*$ state and/or the ground state PES via one (or more) uncharacterized CIs. The former pathway will almost certainly access the $^1(n/\pi)\sigma^*$ PES with different geometries from those reached by direct photoexcitation from the ground state (as suggested by Gavrilov et al.[26] in the case of bare furan). The present experimental data suggests that molecules which couple onto the $^1(n/\pi)\sigma^*$ PES in this way have a greater tendency to avoid the CI at extended R_{S-H} and to follow the adiabatic path to electronically excited 2M,3FTyl($\tilde{A}^2A'$) products. We note that product branching at the corresponding CI in thiophenol has been "tuned" by judicious substitution of the benzene ring (with F, CH_3, and OCH_3 groups in the *para*-position).[6] Such substitution modifies the ground state dihedral angle ϕ, by constructive (or otherwise) π-conjugation effects, and thus the region of the $^1\pi\sigma^*$ PES accessed by vertical excitation and the subsequent evolution toward the CI with the ground state.

The relative yield of slow H atoms from 2M,3FT photolysis increases significantly once $\lambda_{phot} \leq 230$ nm, and dominates TKER spectra measured at $\lambda_{phot} = 210.0$ nm. Such trends mirror that observed with many other heteroaromatic systems (e.g., imidazole[11] and pyrrole[10]), and appear to be a feature of photodissociations that proceed via a (diabatically bound) intermediate state (here a $^1(n/\pi)\pi^*$ state). As in the previous cases, slow H atoms can be envisaged to arise via several pathways, including unimolecular decay of highly vibrationally excited ground state molecules formed by radiationless transfer from the photoprepared excited state, and/or unintended multiphoton excitation processes. Possible examples of the latter include: decay of "superexcited" states of the parent molecule formed via further photon absorption (either by the photoexcited $^1(n/\pi)\pi^*$ state molecules or vibrationally excited ground state molecules formed by internal conversion), and secondary photolysis of any H-containing products formed during the photolysis laser pulse.

The S−H bond strength in 2M,3FT, determined as 31320 ± 100 cm^{-1}, is very similar to that in H_2S {$D_0(HS-H) = 31440 \pm 20$ cm^{-1} [31]} and comparable to that in methanethiol

$\{D_0(CH_3S-H) = 30250 \pm 100\ cm^{-1}$ [42]$\}$. All three are significantly larger than that in thiophenol $\{D_0(C_6H_5S-H) = 28030 \pm 100\ cm^{-1}$ [7]$\}$. In thiophenol, the equilibrium value of the C−C−S−H dihedral angle $\phi = 0°$ and the S lone pair is weakly conjugated into the benzene π-system. This is reflected in the relatively small energetic separation between the $\tilde{X}$ and $\tilde{A}$ states of the thiophenoxyl radical: $T_{00} = 2800 \pm 40\ cm^{-1}$. Any donation of electron density from the S atom to the ring could have the effect of (i) reducing the residual electron density available for S−H bonding in the parent and (ii) stabilizing the thiophenoxyl radical; both effects will serve to lower the S−H bond strength in the parent molecule. Neither H_2S nor CH_3SH have a conjugated π system to share the S lone pair, and their S−H bond strengths are correspondingly greater. 2M,3FT has a ring π-system, but the S lone pair actually serves to destabilize the π-density, particularly in the radical, thereby increasing the parent S−H bond strength.

6. Conclusions

X−H bond fissions in heteroatom containing aromatic molecules are attracting much current interest in view of the potential photobiochemical relevance of such processes. $^1\pi\sigma^*$ excited states (especially the first such excited state) in these molecules have been singled out for particular attention, since the first $^1\pi\sigma^*$ and ground state PESs exhibit a CI at extended R_{X-H} which might offer a potentially efficient route for radiationless transfer back to the ground state, thereby ensuring photostability. $^1\pi\sigma^*$ states are of interest experimentally, because excitation to such states (in the gas phase, at least) leads to X−H bond fission and offers an unusually well characterized "test-bed" for exploring possible signatures of exit channel CIs on the electronic and vibrational branching in the eventual radical products.

2M,3FT was selected for study because it offers revealing energetic and photochemical similarities and contrasts with another, previously studied,[7] SH decorated aromatic system—thiophenol. Specifically, a combination of experiment and *ab initio* theory show that the energetic ordering of the lowest $^1(n/\pi)\sigma^*$ and $^1(n/\pi)\pi^*$ excited states in these two molecules is reversed, so that photoabsorption allows direct access to the former state in 2M,3FT. Vertical excitation prepares 2M,3FT molecules in the $^1(n/\pi)\sigma^*$ state with their S−H bond directed out of the plane of the furan ring, but the minimum energy dissociation pathway on this excited state PES encourages planarity and extension of R_{S-H}. The dissociating molecules evolve through the CI linking the $^1(n/\pi)\sigma^*$ and ground state PESs at planar geometries and follow the diabatic route to H + 2M,3FTyl($\tilde{X}^2A''$) radical products. The H atoms display (non-limiting) perpendicular recoil anisotropy, and the partner radicals are formed in just a few of their lowest vibrational levels. Such energy disposal is understandable, given the forces acting on the nuclear framework as the molecules evolve on the $^1(n/\pi)\sigma^*$ PES. In this regard, 2M,3FT can thus be viewed as an S-based analogue of imidazole, in which the $^1\pi\sigma^*$ state can also be populated directly at long λ_{phot}, and the subsequent N−H bond fission displays similarly uncomplicated dynamics.

The parent absorption cross section of 2M,3FT increases at shorter λ_{phot} (~230 nm). Excitation at these wavelengths is deduced to populate one or more $^1(n/\pi)\pi^*$ excited states which dissociate after radiationless transfer to the $^1(n/\pi)\sigma^*$ and/or ground state PES. Dissociations via the former pathway appear to show a propensity for forming electronically excited 2M,3FTyl($\tilde{A}^2A'$) products, while molecules that couple to high vibrational levels of the ground state are assumed to contribute to the yield of slow H atoms which dominates the TKER spectra obtained at short λ_{phot}.

As in thiophenol, geometry changes in the heavy atom frame accompanying photoexcitation of 2M,3FT to its $^1(n/\pi)\sigma^*$ state and its subsequent S−H bond fission can be understood in terms of the evolving conjugation of the S(3*p*) lone pair orbital and the ring π-system. The two systems show notable differences, however. In ground state thiophenol, and in the eventual thiophenoxyl radicals, the SH group lies in the ring plane. The S(3*p*) lone pair orbital lies along the *x*-axis, and is conjugated with the benzene π-system. As shown previously,[6] the extent of this conjugation can be influenced further by judicious substitution. 2M,3FT, in contrast, has six π-electrons distributed over five heavy atoms and, simplistically, can be viewed as being "electron rich". Conjugation with the S(3*p*) lone pair would tend to destabilize the ground state molecule, an effect that is minimized by aligning the S lone pair near orthogonal to the π-system of the furan ring. Upon photoexcitation, however, a π-hole is created in the ring system and the minimum energy configuration is now achieved by orienting the S(3*p*) lone pair to allow conjugation into the ring, thereby stabilizing the π-hole. Changing the ring attached to the SH group (from benzene to furan) thus has the effect of tuning the extent of conjugation between the S lone pair and the ring π-system. This conjugative effect, together with the increased energy separation of the ring localized π and π^* orbitals in furan (compared with benzene), ensures that the dissociative $^1(n/\pi)\sigma^*$ state is the lowest energy excited state in 2M,3FT.

Acknowledgment. The authors are grateful to EPSRC, for the award of programme grant, and to J. N. Harvey, F. R. Manby, K. N. Rosser, J. M. Beames, and P. N. A. Gunn for their many and varied contributions to this work.

References and Notes

(1) Ashfold, M. N. R.; Devine, A. L.; Dixon, R. N.; King, G. A.; Nix, M. G. D.; Oliver, T. A. A. *Proc. Natl. Acad. Sci.* **2008**, *105*, 12701.
(2) Ashfold, M. N. R.; Cronin, B.; Devine, A. L.; Dixon, R. N.; Nix, M. G. D. *Science* **2006**, *312*, 1637.
(3) Hause, M. L.; Yoon, Y. H.; Case, A. S.; Crim, F. F. *J. Chem. Phys.* **2008**, *128*, 104307.
(4) Iqbal, A.; Cheung, M. S. Y.; Nix, M. G. D.; Stavros, V. G. *J. Phys. Chem. A* **2009**, *113*, 7984.
(5) Lim, I. S.; Lim, J. S.; Lee, Y. S.; Kim, S. K. *J. Chem. Phys.* **2007**, *126*, 034306.
(6) Lim, J. S.; Lee, Y. S.; Kim, S. K. *Angew. Chem., Int. Ed.* **2008**, *47*, 1853.
(7) Devine, A. L.; Nix, M. G. D.; Dixon, R. N.; Ashfold, M. N. R. *J. Phys. Chem. A* **2008**, *112*, 9563.
(8) Blank, D. A.; North, S. W.; Lee, Y. T. *Chem. Phys.* **1994**, *187*, 35.
(9) Wei, J.; Kuczmann, A.; Riedel, J.; Renth, F.; Temps, F. *Phys. Chem. Chem. Phys.* **2003**, *5*, 315.
(10) Cronin, B.; Nix, M. G. D.; Dixon, Qadiri, R. H.; Ashfold, M. N. R. *Phys. Chem. Chem. Phys.* **2004**, *6*, 5031.
(11) Devine, A. L.; Cronin, B.; Nix, M. G. D.; Ashfold, M. N. R. *J. Chem. Phys.* **2006**, *125*, 184302.
(12) Nix, M. G. D.; Devine, A. L.; Cronin, B.; Ashfold, M. N. R. *Phys. Chem. Chem. Phys.* **2006**, *8*, 2610.
(13) Nix, M. G. D.; Devine, A. L.; Cronin, B.; Ashfold, M. N. R. *J. Chem. Phys.* **2007**, *126*, 124312.
(14) Sobolewski, A. L.; Domcke, W. *Chem. Phys.* **2000**, *259*, 181.
(15) Flicker, W. M.; Mosher, O. A.; Kuppermann, A. *J. Chem. Phys.* **1976**, *64*, 1315.
(16) Roebber, J. L.; Gerrity, D. P.; Hemley, R.; Vaida, V. *Chem. Phys. Lett.* **1980**, *75*, 104.
(17) Cooper, C. D.; Williamson, A. D.; Miller, J. C.; Compton, R. N. *J. Chem. Phys.* **1980**, *73*, 1527 (and references therein).
(18) Palmer, M. H.; Walker, I. C.; Ballard, C. C.; Guest, M. F. *Chem. Phys.* **1995**, *192*, 111 (and references therein).
(19) Ridley, T.; Lawley, K. P.; Donovan, R. J. *Phys. Chem. Chem. Phys.* **2004**, *6*, 5304.
(20) Philis, J. G. *Spectrochim. Acta, Part A* **2007**, *67*, 1357.

(21) Sorkabi, O.; Qi, F.; Rizvi, A. H.; Suits, A. G. *J. Chem. Phys.* **1999**, *111*, 100.
(22) Serrano-Andrés, L.; Merchán, M.; Nebot-Gil, I.; Roos, B.; Fülscher, M. *J. Am. Chem. Soc.* **1993**, *115*, 6184.
(23) Nakano, H.; Tsuneda, T.; Hashimoto, T.; Hirao, K. *J. Chem. Phys.* **1996**, *104*, 2312.
(24) Gromov, E. V.; Trofimov, A. B.; Vitkovskaya, N. M.; Chirmer, J.; Köppel, H. *J. Chem. Phys.* **2003**, *119*, 737.
(25) Christiansen, O.; Jørgensen, P. *J. Am. Chem. Soc.* **1998**, *120*, 3423.
(26) Gavrilov, N.; Salzmann, S.; Marian, C. M. *Chem. Phys.* **2008**, *349*, 269.
(27) Wan, J.; Meller, J.; Hada, M.; Ehara, M.; Nakatsuji, H. *J. Chem. Phys.* **2000**, *113*, 7853.
(28) Kerscher, R.; Grosch, W. *J. Agric. Food Chem.* **1998**, *46*, 1954.
(29) Giuliani, A.; Delwiche, J.; Hoffmann, S. V.; Limão-Vieira, P.; Mason, N. J.; Hubin-Franskin, M.-J. *J. Chem. Phys.* **2003**, *119*, 3670.
(30) Philis, J. G.; Melissas, V. S. *Chem. Phys.* **2007**, *336*, 136.
(31) Wilson, S. H. S.; Howe, J. D.; Ashfold, M. N. R. *Mol. Phys.* **1996**, *88*, 841.
(32) Cook, P. A.; Langford, S. R.; Dixon, R. N.; Ashfold, M. N. R. *J. Chem. Phys.* **2001**, *114*, 1672.
(33) Huber, K.-P.; Herzberg, G. *Constants of Diatomic Molecules*; Van Nostrand Reinhold: New York, London, 1979.
(34) Frisch, M. J.; Trucks, G. W.; Schlegel, H. B.; Scuseria, G. E.; Robb, M. A.; Cheeseman, J. R.; Montgomery, J. A., Jr.; Vreven, T.; Kudin, K. N.; Burant, J. C.; Millam, J. M.; Iyengar, S. S.; Tomasi, J.; Barone, V.; Mennucci, B.; Cossi, M.; Scalmani, G.; Rega, N.; Petersson, G. A.; Nakatsuji, H.; Hada, M.; Ehara, M.; Toyota, K.; Fukuda, R.; Hasegawa, J.; Ishida, M.; Nakajima, T.; Honda, Y.; Kitao, O.; Nakai, H.; Klene, M.; Li, X,; Knox, J. E.; Hratchian, H. P.; Cross, J. B.; Adamo, C.; Jaramillo, J.; Gomperts, R.; Stratmann, R. E.; Yazyev, O.; Austin, A. J.; Cammi, R.; Pomelli, C.; Ochterski, J. W.; Ayala, P. Y.; Morokuma, K.; Voth, G. A.; Salvador, P.; Dannenberg, J. J.; Zakrzewski, V. G.; Dapprich, S.; Daniels, A. D.; Strain, M. C.; Farkas, O.; Malick, D. K.; Rabuck, A. D.; Raghavachari, K.; Foresman, J. B.; Ortiz, J. V.; Cui, Q.; Baboul, A. G.; Clifford, S.; Cioslowski, J.; Stefanov, B. B.; Liu, G.; Liashenko, A.; Piskorz, P.; Komaromi, I.; Martin, R. L.; Fox, D. J.; Keith, T.; Al-Laham, M. A.; Peng, C. Y.; Nanayakkara, A,; Challacombe, M.; Gill, P. M. W.; Johnson, B.; Chen, W.; Wong, M. W.; Gonzalez C.; Pople, J. A. *Gaussian 03*, revision B.04; Gaussian, Inc.: Pittsburgh, PA, 2003.
(35) Werner, H. J.; Knowles, P. J.; Lindh, R.; Manby, F. R.; Schütz, M.; Celani, P.; Korona, T.; Rauhut, G.; Amos, R. D.; Bernhardsson, A.; Berning, A.; Cooper, D. L.; Deegan, M. J. O.; Dobbyn, A. J.; Eckert, F.; Hampel, C.; Hetzer, G. Lloyd, A. W.; McNicholas, S. J.; Meyer, W.; Mura, M. E.; Nicklass, A.; Palmieri, P.; Pitzer, R.; Schumann, U.; Stoll, H.; Stone, A. J.; Tarroni, R.; Thorsteinsson, T. *MOLPRO, a package of ab initio programs*, version2006.1; Cardiff, U.K., 2006.
(36) Roos, B. O.; Andersson, K. *Chem. Phys. Lett.* **1995**, *245*, 215.
(37) Barbatti, M.; Lischka, H.; Salzmann, S.; Marian, C. M. *J. Chem. Phys.* **2009**, *130*, 034305.
(38) Beames, J. M.; Nix, M. G. D.; Hudson, A. J. *J. Chem. Phys.*, submitted for publication.
(39) Ahlrichs, R.; Bär, M.; Häser, M.; Horn, H.; Kölmel, C. *Chem. Phys. Lett.* **2001**, *162*, 165.
(40) Nyulászi, L.; Várnai, P.; Veszprémi, T. *J. Mol. Struct.* **1995**, *358*, 55.
(41) Chen, X.; Wu, F.; Yan, M.; Li, H.-B.; Tian, S. X.; Shan, X.; Wang, K.; Li, Z.; Xu, K. *Chem. Phys. Lett.* **2009**, *472*, 19.
(42) Wilson, S. H. S.; Ashfold, M. N. R.; Dixon, R. N. *J. Chem. Phys.* **1994**, *101*, 7538.
(43) Chen, Z.; Shuai, Q.; Jiang, B.; Parker, D.; Yang, X. Unpublished results.
(44) Nourbakhsh, S.; Yin, H.-M.; Liao, C.-L.; Ng, C. Y. *Chem. Phys. Lett.* **1992**, *190*, 469.
(45) Herzberg, G. *Infrared and Raman Spectra of Polyatomic Molecules*; van Nostrand: Princeton, NJ, 1945.

JP905784F